Eur Biophys J (2001) 30: 140–146
DOI 10.1007/s002490100132

ARTICLE

R. Tóth-Boconádi · A. Dér · S. G. Taneva
N. P. Tuparev · L. Keszthelyi

Buffer effects on electric signals of light-excited bacteriorhodopsin mutants

Received: 17 July 2000 / Revised version: 2 November 2000 / Accepted: 20 December 2000 / Published online: 15 March 2001

Abstract The effects of glycyl-glycine and bis-tris-propane buffers on the light-excited electric signals due to proton motion in the molecule were studied for the bacteriorhodopsin (bR) mutants D38R, D96N, E204Q, R227Q, D85N, D85T, R82Q/D85N, and D85N/D96N in purple membranes and for delipidated purple membrane containing the wild-type bR. The results show additional charge motion caused by the buffers in all cases. Arrhenius parameters calculated from the temperature dependence of the difference signals (with buffer minus without buffer) are similar to the parameters found for the wild-type bR in the case of these buffers: the values of the activation enthalpies are mostly in the range 25–50 kJ/mol; all the activation entropies are negative. The results are evaluated with the cluster hypothesis outlined previously.

Keywords Purple membrane · Orientation · Proton pump · Activation enthalpy · Activation entropy

Introduction

Different buffers modify the electric signals evoked by proton motion inside the light-excited bacteriorhodopsin (bR) from *Halobacterium salinarum*. Liu et al. (1991) found ''positive'' and ''negative'' buffers that influenced the B_2 component of the electric signal (this corresponds to the L→M transition in the bR photocycle) with positive or negative additional current, respectively. Signal directions are assigned in relation to the direction of proton translocation: a positive signal means charge motion coinciding with it. Among the investigated 31 buffers, the majority produced positive additional components. These are the ''positive'' buffers, and those producing negative additional components are the ''negative'' buffers.

In our previous paper (Tóth-Boconádi et al. 2000) we presented an extension of this work. We measured all components of the electric signals depending on temperature for a ''positive'' buffer, glycyl-glycine (Gly-Gly), and a ''negative'' buffer, bis-tris-propane (BTP), in the case of the wild-type bR. We found a ca. 2-fold increase of the current during continuous illumination and of the translocated charge for flash illumination in the case of Gly-Gly buffer and a decrease and change of sign to ca. –0.5 for the BTP buffer. These changes did not depend on temperature and occurred only at special buffer concentrations and pH in low salt solutions. Arrhenius parameters from the evaluation of the kinetics of the additional signals exhibited activation enthalpies of 35–40 kJ/mol and negative activation entropies.

Because the buffer effects could not be understood using the prevailing hypotheses (Liu et al. 1991; Heberle and Dencher 1992; Heberle et al. 1994; Alexiev et al. 1995) we introduced the ''cluster hypothesis'' (Tóth-Boconádi et al. 2000). In this hypothesis we assume that protons are released by the proton release cluster at the extracellular (EC) side and are taken up by the proton uptake cluster at the cytoplasmic (CP) side. The protonation of the key amino acid Asp85 reorganizes the clusters for the process of proton release and uptake. The measured Arrhenius parameters correspond to these transitions. The other element of the hypothesis is that the released and to be taken up protons move along the charged buffer gradients evoked by the charged surfaces of the purple membrane (pm). The buffer molecules whose charge changed owing to protonation or deprotonation also move to a new position. These two charge motions make up the buffer-induced additional currents. It seemed obvious to study the buffer effects on

R. Tóth-Boconádi · A. Dér · S. G. Taneva
N. P. Tuparev · L. Keszthelyi (✉)
Institute of Biophysics, Biological Research Centre
Hungarian Academy of Sciences, 6701 Szeged, Hungary
E-mail: kl@nucleus.szbk.u-szeged.hu
Fax: +36-62-433133

S. G. Taneva · N. P. Tuparev
Institute of Biophysics,
Bulgarian Academy of Sciences, Sofia, Bulgaria

pm-containing bR mutants with exchanged amino acids in the release or uptake clusters and also on delipidated pm containing wild-type bR.

In this paper we report that the buffers Gly-Gly and BTP change the current for all of the studied species by adding or subtracting additional components to the photoelectric signals recorded without buffer. The electric signals for delipidated membrane with wild-type bR and mutated in the CP clusters were similar to those found for wild-type bR; mutation at the EC side caused quite different signals. The Arrhenius parameters calculated from the temperature dependence of these components are in a range similar to those found for the wild-type bR.

Materials and methods

The pm with the D85T mutant was separated from a strain of the bacterium donated by R.A. Bogomolni. The pm with the mutant D38R was donated by R. Needleman. All pms containing the other mutants expressed in *Halobacterium salinarum* strain L-33 were supplied by J.K. Lanyi. The delipidated pm was prepared as described by Szundi and Stoeckenius (1987). The preparation of the oriented and immobilized membrane samples, the measuring system, and data collection were the same as described by Tóth-Boconádi et al. (2000). The bathing solutions with and without buffers were the same for all mutants, to allow a meaningful comparison. Therefore, no attempt was made to optimize the buffer concentration and pH.

The electric signals, as recorded, are proportional to the current; the time integrals of the currents are proportional to the translocated charge. The absorbed laser light heats up the samples, increasing their conductivity. A small, unavoidable, voltage difference between the electrodes, therefore, induces a small current, constant for a long time (more than 1 s). Working with non-pumping or weakly pumping mutants, a correction was necessary because the integration resulted in a continuously increasing charge versus time curve. The method was to determine the average amplitude of the current outside the time range of the actual electric signal and subtract this value from the total signal. In this way the charge versus time curves ended in constant values.

The electric current was detected with platinized Pt electrodes, as previously. In some cases the light absorption changes were checked as in Tóth-Boconádi et al. (2000).

Results

Flash excited photoelectric signals in different time and amplitude regions were recorded for all mutants and for the delipidated pm at four temperatures between 8 and 30 °C. The results of this study could be divided into three groups according to mutation. In group 1 are the delipidated pms containing wild-type bR and D38R, D96N, and R227Q modified at the CP side. E204Q modified in the EC side belongs to group 2. The mutants D85N, D85T, R82Q/D85N, and D85N/D96N, that do not pump protons under the established circumstances, are in group 3. In the following, a few of the recorded signals are presented.

Delipidated pm and mutants D38R, D96N, and R227Q

The electric responses of bR in the delipidated pm are nearly the same as the bR in the non-delipidated pm; thus we present only the numerical results in Table 1,

Table 1 Arrhenius parameters for the rise and decay of the buffer-induced signals. The activation enthalpy (ΔH) and activation entropy (ΔS) values are in kJ/mol and kJ/mol K, respectively. Errors smaller than 10–15% of the values are not given

Mutant	Gly-Gly		BTP	
	ΔH	ΔS	ΔH	ΔS
Rise				
Wild-type	37	−0.041	36	−0.040
Wild-type DL[a]	32	−0.052	37	−0.033
Wild-type D_2O	28	−0.08	36	−0.053
D38R	41	−0.011	33	−0.037
D96N	36	−0.04	38	−0.04
R227Q	28	−0.073	33	−0.052
E204Q	25	−0.03	39	−0.054
D85N	45	−0.022	–[b]	–[b]
D85T	44	−0.066	45	−0.022
R82Q/D85N	44	−0.017	47	−0.005
D85N/D96N	30	−0.058	30	−0.070
Decay				
Wild-type	42	−0.031	41	−0.033
Wild-type DL[a]	43	−0.034	42	−0.039
Wild-type D_2O	40	−0.052	39	−0.066
D38R	35.3	−0.059	41	−0.037
D96N	38	−0.05	41	−0.04
R227Q	28	−0.073	33	−0.052
E204Q	52	−0.030	43	−0.063
D85N	51	−0.015	43	−0.037
D85T	41	−0.048	30	−0.090
R82Q/D85N	32	−0.091	44	−0.033
D85N/D96N	28	−0.075	46	−0.028

[a] Delipidated pm
[b] Not determined

which also contains the parameters for wild-type bR in H_2O and D_2O solutions.

D38R, D96N, and R227Q pump protons but with a long lifetime. The long lifetimes are due in the case of D38R to the amino acid arginine of high p*K* introduced at the cytoplasmic (CP) side of bR (Riesle et al. 1996; Checover et al. 1997). Figure 1 shows the current curves and Fig. 2 the time integrals. It is seen that the buffer Gly-Gly creates a positive additional component and BTP creates a negative additional component. The time-integrated curves, proportional to the translocated charge, in Fig. 2 demonstrate that the buffer Gly-Gly increases the translocated charge, while the buffer BTP reverses and decreases it.

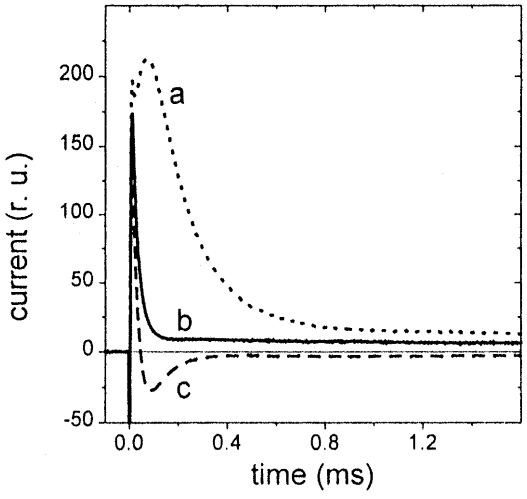

Fig. 1 Electric signals measured in the presence of Gly-Gly (curve *a*) and BTP (curve *c*) buffers and without buffers (curve *b*) in the case of D38R mutant. Buffer concentration: 5 mM Gly-Gly, 1 mM BTP, respectively; pH 7.5, temperature 30 °C. Both bathing solutions contained 50 μM $CaCl_2$

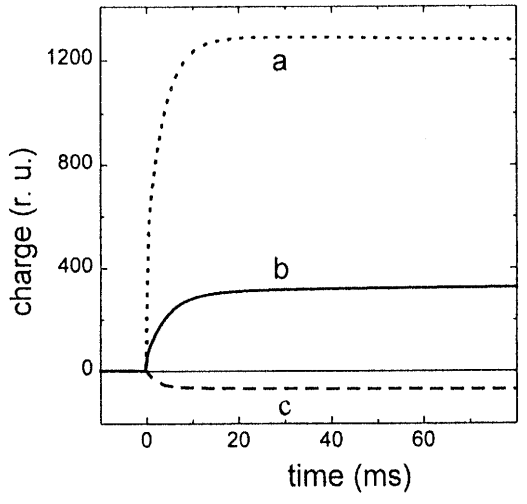

Fig. 2 Time integrated electric signals measured in the presence of Gly-Gly (curve *a*) and BTP (curve *c*) buffers and without buffers (curve *b*) in the case of the D38R mutant. Parameters as in Fig. 1

In the case of pm containing the mutant D96N, the photocycle and the proton transport have long lifetimes (Butt et al. 1989). The electric responses are similar to those for D38R; thus we present the numerical results only in Table 1.

The presence of the Gly-Gly buffer induces positive additional components and the BTP buffer induces negative additional components in the case of the mutant R227Q. The relevant data are collected in Table 1.

Mutant E204Q

The important characteristic of the mutant E204Q is that the proton emission essentially slows down because Glu204, part of the proton releasing cluster at the EC side (Brown et al. 1995; Dioumaev et al. 1998), is not available for the proton relay. The time dependencies of the currents (Fig. 3) and the transported charge (Fig. 4) reflect this slow proton emission. The positive effect of the Gly-Gly buffer and the negative effect of the BTP buffer are also seen.

The protein electric response signal of this mutant in the buffer-free case contains an unusual negative component in the microsecond time domain, indicating that after the deprotonation of the Schiff base, i.e. after proton transport to Asp85, represented by the first positive component, charges move backward. This is demonstrated in Fig. 5 (solid line), together with the effect of the buffers that influence these electric responses. In this figure the first negative signal is not shown; the first positive signal is truncated in order to see the unusual second negative component. The effect of buffers in this time range is opposite to the effects in the millisecond time range (Fig. 3): Gly-Gly pushes the signal to a negative direction and BTP to a positive direction.

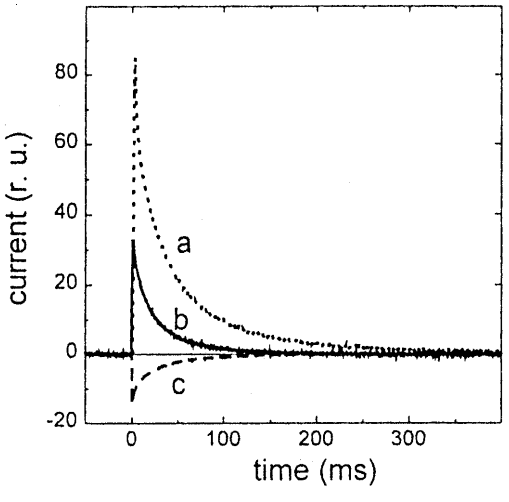

Fig. 3 Electric signals measured in the presence of Gly-Gly (curve *a*) and BTP (curve *c*) buffers and without buffers (curve *b*) in the case of the E204Q mutant. Buffer concentration: 5 mM Gly-Gly, 1 mM BTP, respectively; pH 7.5, temperature 30 °C. Both bathing solutions contained 50 μM $CaCl_2$

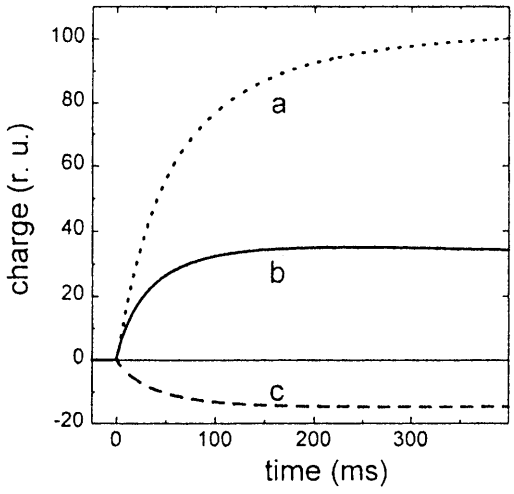

Fig. 4 Time integrated electric signals measured in the presence of Gly-Gly (curve *a*) and BTP (curve *c*) buffers and without buffers (curve *b*) in the case of the E204Q mutant. Parameters as in Fig. 3

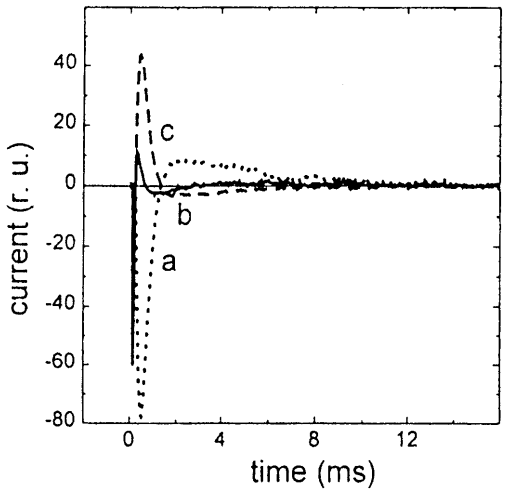

Fig. 6 Electric signals measured in the presence of Gly-Gly (curve *a*) and BTP (curve *c*) buffers and without buffers (curve *b*) in the case of the D85N mutant. Buffer concentrations: 5 mM Gly-Gly, 1 mM BTP, respectively; pH 7.5, temperature 28 °C. Both bathing solutions contained 50 μM $CaCl_2$

Mutants D85N, D85T, R82Q/D85N, and D85N/D96N

The main characteristic of these mutants is that they do not pump protons in the given circumstances. Thus, electric signals due to the interactions of released protons and buffers are not expected. In Fig. 6 the current signals for the mutant D85N are presented. The signals in the case of the mutant D85T are very similar (not shown). It is interesting to note that the current curves, even in buffer-free cases, have three components: the first negative signal is followed by a second positive and a third negative component of longer lifetime. We interpret these signals as a three-step charge motion: first backward (as general for all mutants), then forward but beyond its place in the ground state, and in the third step the charge returns to the original position (Fig. 7). The effect of Gly-Gly buffer is a negative additional component in the short time range and a positive component in the long time range. The situation is just opposite in the case of BTP buffer: a positive additional component appears in the short time range followed by a negative component of long lifetime. Thus, it is certain that noticeable buffer effects are also present for these mutants.

The charge curves (Fig. 8) were obtained after correction for a temperature effect, as pointed out in Materials and methods. The data for mutant D85T are similar.

We checked the changes of light absorption after excitation, with both buffers and without them, at three wavelengths (400, 570, and 650 nm, not shown). The time constants are practically the same with and without buffers. Absorption changes at 400 nm, characteristic for proton pumping, are absent.

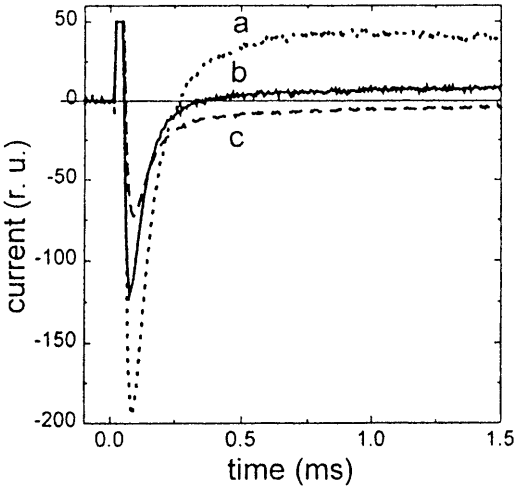

Fig. 5 Electric signals measured in the presence of Gly-Gly (curve *a*) and BTP (curve *c*) buffers and without buffers (curve *b*) in the case of the E204Q mutant in the microsecond time domain. Parameters as in Fig. 3

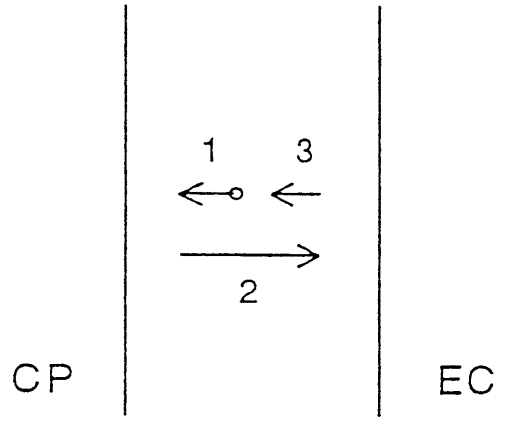

Fig. 7 Sketch of charge motion during the photocycle in the D85 mutant

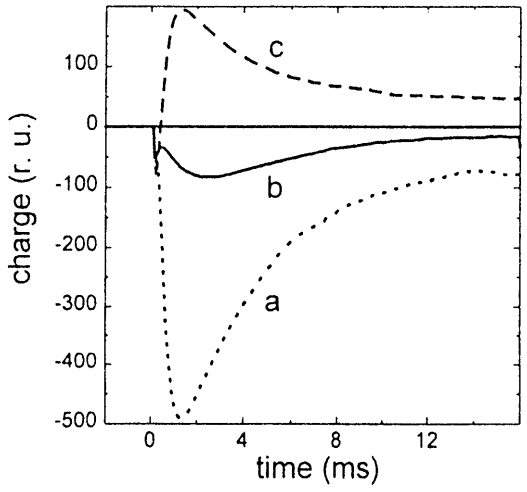

Fig. 8 Time integrated electric signals measured in the presence of Gly-Gly (curve *a*) BTP (curve *c*) and without buffers (curve *b*) in the case of the D85N mutant. Parameters as in Fig. 6

The mutation D85N is also the main determinant of the charge motion in the double mutants R82Q/D85N and D85N/D96N. The second mutation, however, changes the electric responses of these mutants, distinguishing them from the single mutants D85N and D85T. They, seemingly, do not have a pronounced negative component with a longer lifetime. We show this for the mutant R82Q/D85N in Fig. 9 for both buffers. The additional currents due to the buffers have negative signs but differ in amplitudes. The double mutant D85N/D96N behaves similarly.

Discussion

Our goal was not to study the photoelectric signals of the different mutants without the buffers and to analyse them together with optical data. We note, however, that the photoelectric signals are in good agreement with those already published for R227Q (Drachev et al. 1992), for E204Q (Kalaidzidis et al. 1998), for D85N and D96N (Gergely and Váró 1992; Gergely et al. 1993; Tittor et al. 1994), and for D85T and D85N/D96N (Tittor et al. 1994). We think that the electric responses for light excitation of mutants D38R and R82Q/D85N were recorded first in our study. Nevertheless, only the difference curves (signals with buffer minus those without buffer) were analysed.

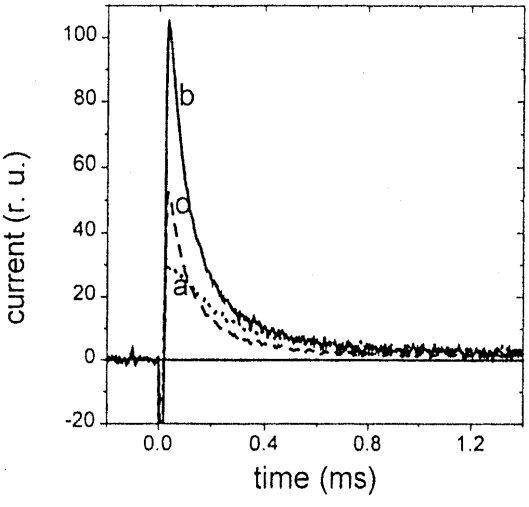

Fig. 9 Electric signals measured in the presence of Gly-Gly (curve *a*) and BTP (curve *c*) and without buffer (curve *b*) in the case of the R82Q/D85N double mutant. Buffer concentrations: 5 mM Gly-Gly, 1 mM BTP, respectively; pH 7.5, temperature 23 °C. Both bathing solutions contained 50 μM $CaCl_2$

From the temperature dependence of the lifetime values of the difference curves, the activation enthalpies and entropies were calculated. These values are in Table 1. The parameters for the wild-type bR in H_2O and D_2O (Tóth-Boconádi et al. 2000) are also included.

The main result of these calculations is that the activation enthalpies of the first two components of the additional electric signals are in the range 25–50 kJ/mol and all of the activation entropies are negative (Table 1). Consequently, it can be accepted that the buffer effects occurring in the electric signals of these mutants are more or less similar.

The time dependencies of the additional current for the buffers are similar in the microsecond time range for wild-type bR in different conditions, and for the mutants in the group 1 [Figs. 1 and 8 in our previous paper (Tóth-Boconádi et al. 2000) and Fig. 1 in the present paper]. On the other hand, mutation in the EC cluster (E204Q) alters the time course of the additional currents completely. The characteristic forms in the microsecond range are absent, but a delayed rise and long-living decay appear (Figs. 3 and 4). Nevertheless, the activation enthalpies determined from the difference curves are in the usual range and the activation entropies are negative, indicating that similar rearrangements may occur also in this mutant.

The exchanged amino acids in all other mutants, D85N and D85T, and in the double mutants, R82Q/D85N and D85N/D96N, are in the neighbourhood of the Schiff base. The charges of R82 (positive) and D85 (negative) play an important role in the first steps of the bR photocycle (Butt et al. 1989; DeGroot et al. 1989, 1990; Dér et al. 1991; Tittor et al. 1994; Luecke et al. 1999). The time-integrated curves tend to zero (Fig. 8) because of the absence of proton pumping activity.

The additional charge motions seem to be different in the case of the different non-pumping mutants (Figs. 6 and 9). We define the additional charge motion (ACHM) as the time-integrated area of the short-living component of the difference of the signals with buffer minus without buffer divided by the area of the first negative signal multiplied by –1. The ACHM data are in Table 2. The near-zero time integrals for these mutants determine that the ACHM values of the longer living components are nearly equal to those in Table 2, but with opposite signs.

We assume that the additional currents are due to the changing charge distribution inside the bR during the

Table 2 Data for the additional charge motion (ACHM) of the first component due to buffers for the non-pumping mutants and for the E204Q pumping mutant in the microsecond time domain

Mutant	Gly-Gly	BTP
E204Q	−3.2	+1.7
D85N	−1.5	+0.65
D85T	−0.18	+0.13
D82Q/D85N	−0.26	−0.24
D85N/D96N	−0.10	−0.54

photocycle and, consequently, to an electric field which acts on the charged buffer molecules being in the neighbourhood of the pm. This is more or less the explanation elaborated by Liu et al. (1991). It is interesting to observe that the Arrhenius parameters are similar to those for pumping and non-pumping mutants. The presumable reason is that the internal charge motions, though proton release is absent, rearrange the clusters that are similar to the proton release and uptake clusters in the pumping mutants.

In the cases of D85N and D85T, the internal charge motions occur mainly in three steps as modelled in Fig. 7: first is the usual fast negative charge motion, second is a positive one, and the ground state is finally reestablished by a negative charge motion. The sketch in Fig. 7 indicates a negative and a positive dipole (looking from the EC side). The first additional component in Gly-Gly buffer is negative, the second positive. The negative charge of the negative dipole repels the negative buffer molecules at the EC side and the positive part attracts them at the CP side, thus producing a negative current. The reversed dipole just does the opposite.

This simple explanation is not sufficient in the case of the positively charged BTP buffer because the negative dipole would induce negative additional current as in the case of Gly-Gly buffer, contrary to the observed positive current. The BTP buffer molecules, being positive at the pH of the measurement, are very near to the pm and therefore they may be driven differently by local electric fields. We assume that the negative charge of the negative dipole looking to the EC side attracts positive ions, producing a negative current, and a local field at the CP side induces a positive current. The positive current from the CP side may be larger than the negative current from the EC side. The sum is the observed positive additional current. We note that the ACHM is smaller for BTP buffer than for the Gly-Gly buffer (Table 2), supporting its origin as a difference of two currents. The reversed dipole in the third step induces the negative additional current.

In the cases of the double mutants, R82Q/D85N and D85N/D96N, the additional currents due to Gly-Gly and BTP have the same negative sign, at least in the time range shown (Fig. 9). It is known that the second mutation changes the characteristics of bR [for example, Tittor et al. (1994) for D85N/D96N and Váró et al. (1996) for T46V/R227Q]. We assume that the internal dipoles produced during the photocycle differ from those with a single mutation.

The additional charge motion in the non-pumping mutants is small compared to the changes of the currents in the case of the pumping mutants. This process, assigned to the motion of the charged buffers, may also occur for pumping mutants. Its contribution, however, is negligible compared to the large additional currents due to the proton release and uptake processes. We consider the additional currents for E204Q in the microsecond time domain before the onset of proton pumping as an indication of this process (Fig. 5). The ACHM values for these mutants are also given in Table 2.

Conclusion

The study of the influence of buffers on the electric signals in different mutants demonstrates that the EC and CP clusters play a determining role in generating additional currents. Modifications in the neighbourhood EC clusters lead to transient charge motion only (non-pumping mutants D85N, D85T, R82Q/D85N, and D85N/D96N) or in the EC clusters detectable transient charge motion and delayed additional current (E204Q). Modifications in the CP clusters (D38R, D96N, and R227Q) produce buffer effects similar to the wild-type bR, though the lifetimes and factors are different. The Arrhenius parameters of all of the additional charge motions are also similar. In this way we may accept that the results with mutants are in agreement with the cluster hypothesis and also substantiate it.

Acknowledgements We are grateful to Prof. J.K. Lanyi for supplying the pms with the bR mutants R227Q, D96N, E204Q, D85N, R82Q/D85N, and D85N/D96N, to Prof. R. Needleman for the pm with mutant D38R, and to Prof. R.A. Bogomolni for the strain containing the mutant D85T. This work has been supported by the Hungarian National Science Fund OTKA T 025236.

References

Alexiev U, Mollaaghbaba R, Scherrer P, Khorana HG, Heyn MP (1995) Rapid long-range proton diffusion along the surface of the purple membrane and delayed proton transfer into the bulk. Proc Natl Acad Sci USA 92:372–376

Brown LS, Sasaki J, Kandori H, Maeda A, Needleman R, Lanyi JK (1995) Glutamic acid 204 is the terminal proton release group at the external surface of bacteriorhodopsin. J Biol Chem 270:27122–27126

Butt HJ, Fendler K, Bamberg E, Tittor J, Oesterhelt D (1989) Aspartic acids 96 and 85 play a central role in the function of bacteriorhodopsin as a proton pump. EMBO J 8:1657–1663

Checover S, Nachliel E, Dencher NA, Gutman M (1997) Mechanism of ptoton entry into the cytoplasmic section of the proton-conducting channel of bacteriorhodopsin. Biochemistry 36:13919–13928

DeGroot HJM, Harbison GS, Herzfeld J, Griffin RG (1989) Nuclear magnetic resonance study of the Schiff base in bacteriorhodopsin: counterion effects on the ^{15}N shift anisotropy. Biochemistry 28:3346–3353

DeGroot HJM, Smith SO, Courtin SO, Winkel J, Van den Berg C, Griffin RG, Lugtenburg J, Herzfeld J (1990) Solid-state ^{13}C NMR study of the low pH forms of bacteriorhodopsin. Biochemistry 29:6873–6883

Dér A, Száraz S, Tóth-Boconádi R, Tokaji Zs, Keszthelyi L, Stoeckenius W (1991) Alternative translocation of protons and halide ions by bacteriorhodopsin. Proc Natl Acad Sci USA 88:4751–4755

Dioumaev AK, Richter HT, Brown LS, Tanio M, Tuzi S, Saito H, Kimura J, Needleman R, Lanyi JK (1998) Existence of a proton transfer chain in bacteriorhodopsin: participation of Glu-194 in the release of protons to the external surface. Biochemistry 37:2496–2506

Drachev LA, Kaulen AD, Khorana HG, Mogi T, Postanogova NV, Skulachev VP, Stern LJ (1992) The role of arginines 82 and 227 in the bacteriorhodopsin photocycle. Photochem Photobiol 55:741–744

Gergely Cs, Váró G (1992) Charge motion in the D85N and D212N mutants of bacteriorhodopsin. In: Rigaud JL (ed) Structures and functions of retinal proteins. (Colloque INSERM vol 221) Libbey Eurotext, Paris, pp 193–196

Gergely Cs, Ganea C, Groma G, Váró G (1993) Study of the photocycle and charge motions of the bacteriorhodopsin mutant D96N. Biophys J 65:2478–2483

Heberle J, Dencher NA (1992) Surface bound optical probes monitor proton translocation and surface potential changes during the bacteriorhodopsin photocycle. Proc Natl Acad Sci USA 89:5996–6000

Heberle J, Riesle J, Thiedemann G, Oesterhelt D, Dencher NA (1994) Proton migration along the membrane surface and retarded surface to bulk transfer. Nature 379:379–382

Kalaidzis IV, Belevich IN, Kaulen AD (1998) Photovoltage evidence that Glu-204 is the intermediate proton donor rather than the terminal proton release group in bacteriorhodopsin. FEBS Lett 434:197–200

Liu SY, Kono M, Ebrey TG (1991) Effect of pH buffer molecules on the light-induced currents from oriented purple membrane. Biophys J 60:204–216

Luecke H, Schobert B, Richter H-T, Cartellier J-P, Lanyi JK (1999) Structural changes in bacteriorhodopsin during ion transport at 2 angstrom resolution. Science 286:255–260

Riesle J, Oesterhelt D, Dencher NA, Heberle J (1996) D38 is an essential part of the proton translocation pathway in bacteriorhodopsin. Biochemistry 35:6635–6643

Szundi I, Stoeckenius W (1987) Effect of lipid surface charges on the purple-to-blue transition of bacteriorhodopsin. Proc Natl Acad Sci USA 84:3681–3684

Tittor J, Schweiger U, Oesterhelt D, Bamberg E (1994) Inversion of proton translocation in bacteriorhodopsin mutants D85N, D85T, and D85/D95N. Biophys J 67:1682–1690

Tóth-Boconádi R, Dér A, Keszthelyi L (2000) Buffer effects on electric signals of light excited bacteriorhodopsin. Biophys J 78:3170–3177

Váró G, Needleman R, Lanyi JK (1996) Protein structural changes at the CP surface is the cause of cooperativity in the bacteriorhodopsin photocycle. Biophys J 70:461–467